



# Intermediate conformation between native $\beta$ -sheet and non-native $\alpha$ -helix is a precursor of trifluoroethanol-induced aggregation of Human Carbonic Anhydrase-II

Preeti Gupta, Shashank Deep\*

Department of Chemistry, Indian Institute of Technology Delhi, Hauz Khas, New Delhi 110016, India



## ARTICLE INFO

### Article history:

Received 24 April 2014

Available online 9 May 2014

### Keywords:

Human carbonic anhydrase II

Trifluoroethanol

Protein aggregation

Amyloid fibril

Partially structured conformation

## ABSTRACT

In the present work, we examined the correlation between 2,2,2-trifluoroethanol (TFE)-induced conformational transitions of human carbonic anhydrase II (HCAII) and its aggregation propensity. Circular dichroism data indicates that protein undergoes a transition from  $\beta$ -sheet to  $\alpha$ -helix on addition of TFE. The protein was found to aggregate maximally at moderate concentration of TFE at which it exists somewhere between  $\beta$ -sheet and  $\alpha$ -helix, probably in extended non-native  $\beta$ -sheet conformation. Thioflavin-T (ThT) and Congo-Red (CR) assays along with fluorescence microscopy and transmission electron microscopy (TEM) data suggest that the protein aggregates induced by TFE possess amyloid-like features. Anilino-8-naphthalene sulfonate (ANS) binding studies reveal that the exposure of hydrophobic surface(s) was maximum in intermediate conformation. Our study suggests that the exposed hydrophobic surface and/or the disruption of the structural features protecting a  $\beta$ -sheet protein might be the major reason(s) for the high aggregation propensity of non-native intermediate conformation of HCAII.

© 2014 Elsevier Inc. All rights reserved.

## 1. Introduction

Misfolding and self-assembly of proteins resulting into amyloid deposition has deleterious consequences through their association with a number of human pathologies. These pathologies range from neurodegenerative disorders (e.g., Alzheimer's disease and Parkinson's disease) to non-neuropathic systemic amyloidosis (e.g., dialysis-related amyloidosis and light-chain amyloidosis) [1,2]. In all of these diseased conditions, amyloid aggregates do not develop directly from native state; rather extensive structural reorganization leading to the formation of partially-structured intermediate(s) precedes fibrillation. In both native structures and completely unfolded states, intermolecular contacts responsible for protein aggregation are impeded. However, a partially folded conformation induced at mild denaturing conditions like low pH, high temperature or the presence of moderate concentrations of alcohols allows the establishment of intermolecular interactions needed for the self-association of polypeptides [3–5]. Despite the importance of these species for the understanding of fibrillation process, the structural requisite of an intermediate to form amyloid is not properly understood.

The aggregation of all types of proteins viz. the natively unfolded proteins ( $\alpha$ -synuclein, A $\beta$ -40) [6,7],  $\alpha$ -helical proteins

(insulin, BSA) [8,9] and  $\beta$ -sheet proteins (transthyretin, Superoxide dismutase,  $\beta$ 2-microglobulin) [10–12] have been reported. For the  $\alpha$ -helical proteins, the transition from native  $\alpha$ -helices to non-native intermolecular  $\beta$ -sheets has been suggested to be a trigger of fibrillation in different conformational diseases [13,14]. It has also been shown that the natively unfolded protein e.g.  $\alpha$ -synuclein goes to amyloid through  $\alpha$ -helical intermediate [15–17]. Few studies of amyloid aggregation in  $\beta$ -sheet proteins have been reported [18,19] but the kind of transition and structural changes that promotes aggregation in such proteins is not completely understood. In this context, it would be important to study the amyloid formation in a  $\beta$ -sheet-rich protein. The subject becomes further important if the structural changes involved with the native protein can be correlated to fibrillation. Against this background, study of the effect of TFE, a known  $\alpha$ -helix inducer, on amyloid forming propensity of HCA-II, a  $\beta$ -rich protein, makes an interesting idea. Since a TFE–water mixture resembles the physiological environment by acting as a membrane-mimic [20,21], understanding the mechanism of protein aggregation in its presence provides invaluable information about the fibrillation process associated with a number of human pathologies.

HCAII is a single domain,  $\beta$ -rich globular protein with a central structural motif consisting of 10 stranded twisted  $\beta$  sheet. Only three short  $\alpha$ -helices are present on its surface. Our results indicate the formation of amyloid-like aggregates by HCAII at moderate

\* Corresponding author. Fax: +91 11 26581102.

E-mail address: [sdeep@chemistry.iitd.ac.in](mailto:sdeep@chemistry.iitd.ac.in) (S. Deep).

concentrations of TFE wherein protein adopts a conformational state between native  $\beta$ -sheet and non-native  $\alpha$ -helix.

## 2. Materials and methods

### 2.1. Materials

Thioflavin-T (ThT) and 2,2,2-trifluoroethanol were obtained from Sigma Aldrich. Congo red was purchased from Acros organics. Unless otherwise mentioned, all solutions were prepared in 20 mM Tris-H<sub>2</sub>SO<sub>4</sub> buffer (pH 7.5). All experiments were performed at 25 °C.

### 2.2. Protein expression and purification

HCAII was expressed in a recombinant strain of *Escherichia coli* (BL21 (DE3)) containing a plasmid encoding the HCAII gene. Purification was carried out via affinity chromatography. Briefly, cells were lysed by sonication and the lysate was placed onto an agarose resin coupled with *p*-(aminomethyl)-benzene-sulfonamide, an HCAII inhibitor. The protein was eluted with 0.4 M sodium azide, 100 mM Tris-HCl, pH 7.0, and the azide was removed by extensive buffer exchanging against 10 mM Tris-HCl, pH 8.0. The protein was, then, buffer exchanged into 10 mM Tris-H<sub>2</sub>SO<sub>4</sub>, pH 7.5. Protein purity and integrity was confirmed by SDS-PAGE and enzymatic activity (PNPA assay), respectively. Protein concentration was determined by using extinction coefficient of 54,000 M<sup>-1</sup>cm<sup>-1</sup> at 280 nm.

### 2.3. CD measurements

Circular dichroism (CD) spectra in both far-UV and near-UV region were obtained by using AVIV circular dichroism spectrometer (Model 420SF, Lakewood, NJ, USA) at 20 °C. All measurements were performed using a 1 mm quartz cell, an averaging time of 20 s, and an average of 3 scans were recorded to generate the data. Protein was assayed at 0.1 mg/ml for far-UV and 0.6 mg/ml for near-UV region in appropriate TFE concentrations.

### 2.4. Dye-binding assays

Protein samples (0.1 mg/ml) were incubated overnight in appropriate concentrations of TFE. Aliquots from the incubated samples were diluted into buffer (20 mM Tris-H<sub>2</sub>SO<sub>4</sub>, pH 7.5) containing 50  $\mu$ M ThT, and adjusted to a final volume of 500  $\mu$ L. Fluorescence spectra of the samples prepared in this way were obtained by using a Varian Cary Eclipse fluorescence spectrophotometer equipped with a peltier-based temperature controller. The excitation wavelength was set at 445 nm, and bandwidths for excitation and emission lights were 5 and 10 nm, respectively. For the Congo red binding assay, absorption spectra of the samples containing 20  $\mu$ M solution of the dye (Congo red) were recorded on a Varian Cary 100 UV-Vis spectrophotometer in the wavelength range of 400–600 nm.

### 2.5. Aggregation kinetics

The kinetic assay was performed at 0.1 mg/ml concentration of protein by monitoring the time dependent changes in the absorbance at 350 nm as well as ThT fluorescence at 486 nm.

### 2.6. Steady-state fluorescence measurements

Intrinsic fluorescence spectra were recorded at a protein concentration of 0.1 mg/ml using an excitation wavelength of

295 nm and emission was collected between 310 nm and 400 nm. The fluorescence of ANS was excited at 350 nm and emission collected between 400 nm and 600 nm.

### 2.7. Attenuated total reflectance-Fourier transform infrared (ATR-FTIR) spectroscopy

The FTIR spectra of native protein and aggregates obtained by incubating protein in 20% TFE overnight were acquired using Cary 600 series FTIR spectrometer (Agilent Technologies). All spectra were recorded with wavenumber resolution of 2 cm<sup>-1</sup>. For each spectrum, 128 interferograms were collected and averaged.

### 2.8. Fluorescence microscopy

10  $\mu$ L of overnight incubated protein samples (0% and 20% TFE) were placed on a glass slide and was air dried for 10 min. A 20  $\mu$ M ThT solution was then added and covered with a glass slip. The slide was then observed at 60 $\times$  magnification under dark field to visualize the ThT fluorescence of clusters of amyloid fiber in an Olympus IX71 fluorescence microscope.

### 2.9. Transmission electron microscopy

TEM images of samples were acquired using a Morgagni 268D transmission electron microscope (FEI Co.). The protein aggregate sample (in 20% TFE) obtained after one week of incubation at 25 °C was diluted 4-fold and placed and dried for 5 min on a Formvar-coated grid. The sample was then negatively stained with 1% (w/v) phosphotungstic acid solution, air-dried, and examined at a voltage of 80-kV.

## 3. Results and discussion

### 3.1. Aggregation kinetics

The aggregation kinetics of HCAII in 20% TFE at 25 °C was followed by monitoring the changes in the absorbance at 350 nm (turbidity measurement) (Fig. 1A). At 0.1 mg/ml protein concentration, HCAII aggregation followed hyperbolic kinetic pattern reaching maximal aggregation after 2 h. Absence of lag phase suggests that protein undergoes downhill polymerization under this condition.

### 3.2. TFE induced aggregates possess amyloid fibril-like features

The amyloid properties of TFE-induced aggregates of HCA-II were explored by examining their staining properties and ultrastructural characteristics through dye-binding assays, fluorescence microscopy, electron microscopy and attenuated total reflection Fourier transform infrared spectroscopy.

Thioflavin-T (ThT), a well-known dye routinely used to characterize amyloid-fibrils, was chosen for tinctorial studies. Thioflavin-T is known to distinguish highly-ordered amyloid-fibrils from amorphous aggregates by specifically binding to cross-beta structure with concomitant enhancement in fluorescence emission intensity [22,23]. The evaluation of aggregation process by measuring Thioflavin-T fluorescence intensity at 486 nm showed a time-dependent increase, which occurred following the same hyperbolic kinetic trace as obtained from turbidity measurements (Fig. 1B).

Fig. 1C shows the comparison of fluorescence emission intensity of ThT of protein samples as a function of TFE concentration. No significant increase in fluorescence emission was detected up-to TFE concentration of 10% (v/v). However, a huge enhancement in fluorescence intensity at 485 nm was observed on further increas-

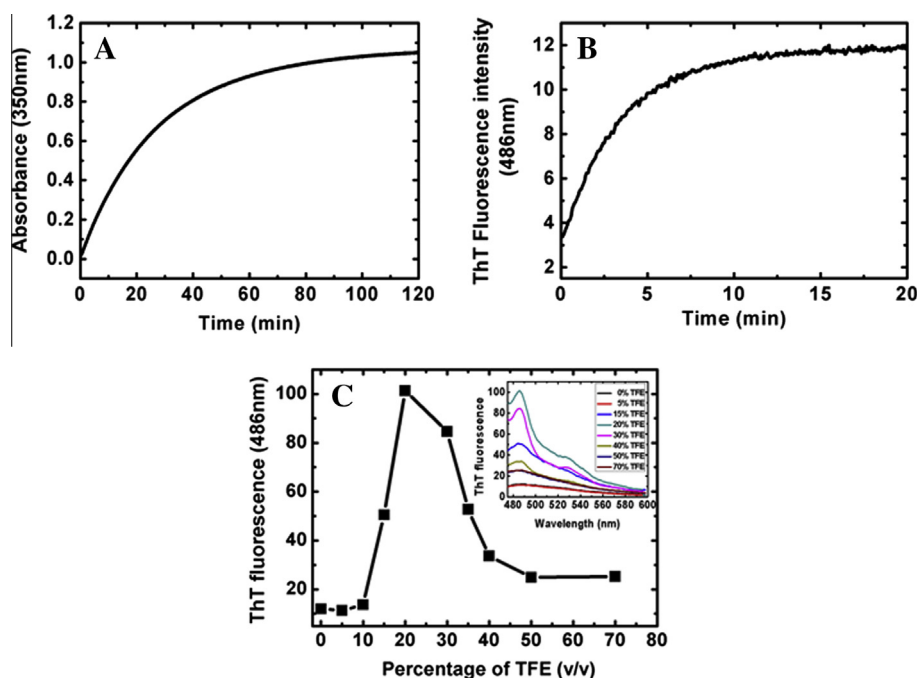


**Fig. 1.** Kinetics of HCAII aggregation in 20% TFE assessed by an increase in (A) absorbance at 350 nm; (B) ThT fluorescence at 486 nm and 25 °C. (C) Changes in fluorescence emission of ThT upon binding to HCAII (0.1 mg/ml) at various concentrations of TFE and 25 °C. Inset: Fluorescence emission spectra of ThT at various concentrations of TFE.

ing the TFE concentration, with a maximum detected at 20% (v/v) TFE. Beyond 20% TFE, a progressive decrease in fluorescence signal was observed. These observations clearly suggest that the aggregation propensity of HCAII is maximum in presence of 20–25% of TFE.

Another amyloid specific dye, Congo red (CR), has an absorbance maximum at 490 nm that increases and undergoes red-shift upon binding to ordered repetitive  $\beta$ -sheet structures in the amyloid fibrils. CR binding of protein aggregates was detected as a characteristic red shifted peak with enhanced absorbance in samples incubated at 20% TFE (v/v) (Fig. S3).

A parallel visualization of the ThT-binding aggregates was done by fluorescence microscopy. The HCA II samples incubated overnight in 20% TFE (v/v) displayed clear visibility due to increased ThT fluorescence in the dark field (Fig. 2A). In contrast no staining was observed with protein alone.

Micrographs obtained by TEM of HCAII aggregates formed in 20% TFE reveal the presence of fibrillar material (Fig. 3A) in addition to amorphous aggregates. The aggregated sample also showed the presence of some ordered beaded structures that might be considered as amyloid precursors (Fig. 2B).

These aggregates were also examined by ATR-FTIR spectroscopy to assess the characteristic polypeptide chain arrangement of aggregated species. The FTIR spectrum of native HCAII was dominated by a peak at  $1635\text{ cm}^{-1}$  which is attributed to the presence of intramolecular  $\beta$ -sheet structure. In contrast, aggregates (in 20% TFE) displayed a shift in absorption peak at  $1619\text{ cm}^{-1}$ , indicative of extensively extended intermolecular  $\beta$ -sheet typical of amyloid like aggregates (Fig. S5).

### 3.3. Partially structured conformations induced at intermediate concentrations of TFE

The secondary structural changes in HCA-II were investigated at various concentrations of TFE using far-UV circular dichroism (CD) spectroscopy. The far-UV CD spectrum of HCA-II showed minima at around 213 nm, characteristic of  $\beta$ -sheet conformation (Fig. 3A). No remarkable change in the CD spectrum was observed at TFE

concentrations up to 10% (v/v), beyond which slight changes occurred in the secondary structural content of the protein up to 30% TFE (Fig. S4). At 20% TFE, CD spectrum obtained is typical of a largely extended non-native  $\beta$ -sheet conformation as revealed by the broad single negative band at around 217 nm. A further increase in TFE concentration results in the induction of new non-native  $\alpha$ -helical conformation as displayed by the two negative ellipticity bands at 208 and 222 nm (Figs. 3A and S4).

Near-UV CD spectra were taken to look at the changes in tertiary structure of protein on addition of TFE. Spectrum of native HCAII showed two major negative ellipticity bands at 282 and 292 nm attributed to the asymmetric structure surrounding the seven tryptophan residues in the protein. No significant changes were observed in the CD spectrum up to 10% TFE. At 20% TFE, the spectrum showed native-like fingerprint but with slightly decreased amplitude of the peaks (Fig. 3B). These lower peak intensities reflect the increased mobility of aromatic side-chains in the conformation induced at intermediate [TFE] as compared to the native protein. Interestingly, at higher TFE concentrations (>50%), the CD spectra showed drastic change owing to the completely different environment around tryptophan residues in the non-native  $\alpha$ -helical conformation (Fig. 3B).

The effect of TFE on the tertiary structure of HCA-II was also evaluated by obtaining intrinsic tryptophan fluorescence spectra. In lieu of near-UV CD spectra, tryptophan fluorescence spectra also do not change significantly up to 10% (v/v) TFE. However, in 20% TFE (v/v), the spectra showed an appreciable increase in fluorescence intensity with a slight blue shift in emission maxima suggesting the perturbation of native tertiary interactions in the protein. At higher TFE concentrations (>50%), the spectra displayed a huge red shift in  $\lambda_{\text{max}}$ , again indicating the change in the local environment of tryptophan residues upon induction of non-native helical conformation in the protein (Fig. 4A).

Our data from CD studies, in conjunction with those obtained from tryptophan fluorescence measurements, suggest that HCA-II exists in partially structured state with increased side chains dynamics at 20% TFE and is different both from the native state

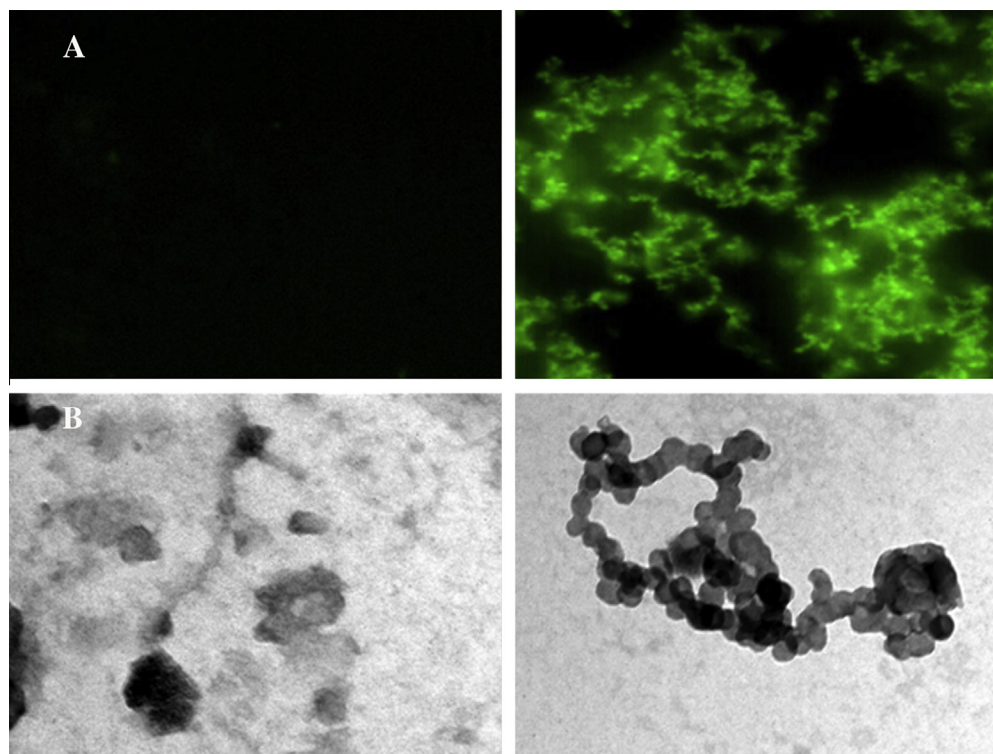


**Fig. 2.** (A) Fluorescence microscopy image of HCAII aggregates after one day of incubation at 0% and 20% TFE. Amyloid stained with ThT was observed in dark field. (B) Electron micrographs of negatively stained HCAII aggregates after incubation at 25 °C for a week in the presence of 20% TFE (scale bar = 200 nm).

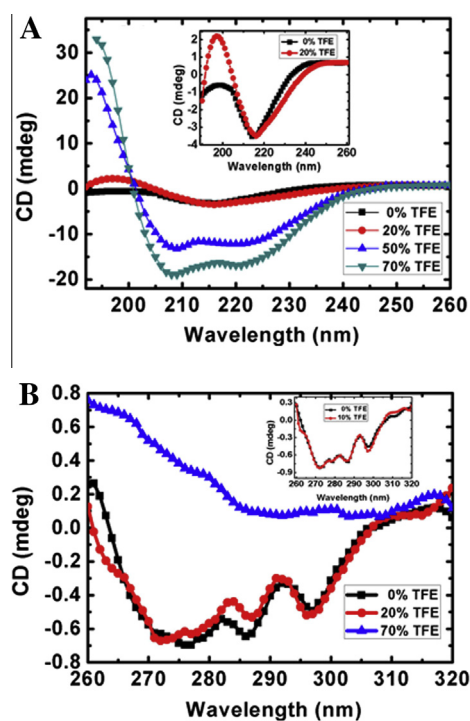


**Fig. 3.** Conformational changes induced by TFE in HCAII monitored by CD spectroscopy (A) Far UV-CD spectra of HCAII at 0%, 20%, 50% and 70% TFE. Inset: Far-UV CD spectra of HCAII at 0% and 20% TFE. (B) Near UV-CD spectra of HCAII at 0%, 20% and 70% TFE. Inset: Near UV-CD spectra of HCAII at 0% and 10% TFE.

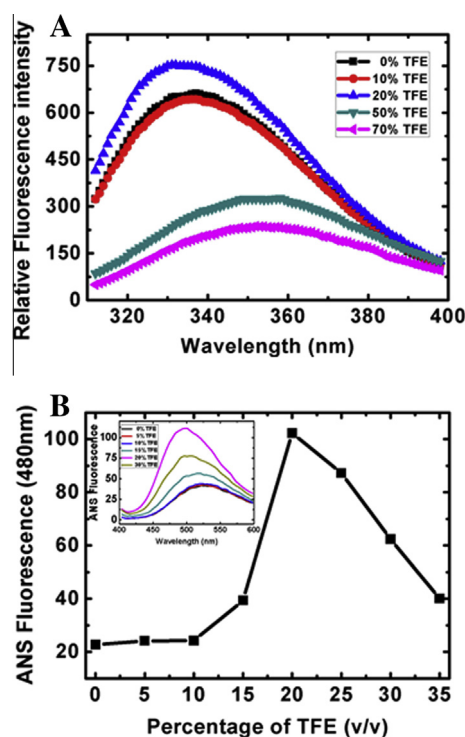


**Fig. 4.** Conformational changes induced by TFE in HCAII monitored by intrinsic and ANS fluorescence emission. (A) HCAII intrinsic emission fluorescence spectra (excitation wavelength was 295 nm) at 0%, 10%, 20% and 70% TFE at 25 °C. (B) Changes in fluorescence emission of ANS (at 480 nm) upon HCAII binding. Inset: Fluorescence emission spectra of ANS upon binding to HCAII (0.1 mg/ml) at various concentrations of TFE after incubation of 12 h at 25 °C. The excitation wavelength was 350 nm.



and non-native  $\alpha$ -helical conformation induced at high concentration of TFE.

#### 3.4. Hydrophobic exposure of conformations at intermediate concentrations of TFE

In order to investigate the nature and accessibility of hydrophobic patches in the conformational states induced by TFE, the polarity-sensitive fluorescent dye aniline-8-naphthalene sulfonate (ANS) was used. With increasing [TFE], the ANS fluorescence spectra showed a prominent blue-shift with increased fluorescent intensity, reaching a maximum value at 20% (v/v) TFE (Fig. 4B). These spectral features clearly indicate the accumulation of partially structured intermediate(s) with exposed hydrophobic surface at intermediate concentration of TFE (maximum at 20% TFE) before the onset of amyloid fibril formation.

#### 4. Discussion

Our work describes the conformational preference of the state induced at intermediate concentration of TFE to form amyloid-like aggregates in a  $\beta$ -sheet rich protein. HCAII aggregation exhibits a bell-shaped dependence on the concentration of fluoroalcohol. At moderate concentrations (15–30%), TFE appears to diminish the tertiary interactions and hydrophobic contacts stabilizing the native structure, thereby, promoting the formation of non-native extended  $\beta$ -sheet conformation with high propensity to aggregate. This partially structured conformation exhibits solvent-exposed hydrophobic patches as evident from its ability to bind ANS. Protein aggregation appears to be triggered by intermolecular contacts between these exposed hydrophobic regions. Another reason for aggregation may be the disruption of proper architecture developed by  $\beta$ -sheet proteins to avoid aggregation. It has been reported that natural  $\beta$ -sheet proteins adopt architecture to prevent edge to edge interaction that promotes aggregation rendering these proteins usually soluble [24]. Any modulation of environment, which alters the key features that have been evolved to protect  $\beta$ -sheet ends, may lead to aggregation. It has been reported that the monomeric  $\beta$ 2-microglobulin shows remarkable structural differences relative to HLA-bound protein. These structural changes are proposed to remove the key features which protect HLA-bound protein to aggregate [25]. In a similar manner, TFE induced conformational changes abolishes such protection allowing the protein to self-assemble and aggregate.

However, at higher concentration of TFE (>50%), the low polarity of solvent hinders the aggregate formation with subsequent stabilization of intermolecular hydrogen bonding network in non-native  $\alpha$ -helical conformation. MD simulation by Roccatano et al. [26] suggests that helix formation effect of TFE is due to preferential binding of TFE to peptide. This leads to displacement of water which provides low dielectric constant that favors the formation of intra-peptide hydrogen bonds. Thus, the intricate balance between hydrophobic interactions and intermolecular hydrogen bonding as well as the polypeptide conformation may be the major driving force in the self-assembly of HCAII.

In summary, human carbonic anhydrase II, a  $\beta$ -sheet protein, can form amyloid-like aggregates in aqueous TFE solutions. TFE concentration and polypeptide backbone conformation are found to be critical for protein aggregation. A moderate concentration of fluoroalcohol favors the formation of partially structured conformation with subsequent aggregation while  $\alpha$ -helical state induced at higher concentrations inhibits aggregation. Our results support the hypothesis that the ability to form amyloid fibrils is a generic property shared by many polypeptide sequences irrespective of any sequence or structure homologies.

#### Acknowledgments

This work is generously supported by the Council for Scientific and Industrial Research (CSIR), Government of India through grants to S.D. and research fellowship to P.G. We thank Dr. Carol Fierke (University of Michigan, Ann Arbor, Michigan) for providing us with the plasmid containing the full length coding region of Carbonic Anhydrase II gene, Dr. Ravikrishnan Elangovan (Indian Institute of Technology, Delhi) for fluorescence microscopy facility and Sophisticated Analytical Instrumentation Facility (AIIMS, Delhi) for transmission electron microscopy, respectively.

#### Appendix A. Supplementary data

Supplementary data associated with this article can be found, in the online version, at <http://dx.doi.org/10.1016/j.bbrc.2014.04.160>.

#### References

- [1] C.M. Dobson, The structural basis of protein folding and its links with human disease, *Philos. Trans. R. Soc. Lond. B: Biol. Sci.* 356 (2001) 133–145.
- [2] P.T. Lansbury Jr., Evolution of amyloid: what normal protein folding may tell us about fibrillogenesis and disease, *Proc. Natl. Acad. Sci. USA* 96 (1999) 3342–3344.
- [3] J.W. Kelly, The environmental dependency of protein folding best explains prion and amyloid diseases, *Proc. Natl. Acad. Sci. USA* 95 (1998) 930–932.
- [4] V.J. McParland, N.M. Kad, A.P. Kalverda, A. Brown, P. Kirwin-Jones, M.G. Hunter, M. Sunde, S.E. Radford, Partially unfolded states of  $\beta$ 2-microglobulin and amyloid formation in vitro, *Biochemistry* 39 (2000) 8735–8746.
- [5] V.N. Uversky, J. Li, A.L. Fink, Evidence for a partially folded intermediate in  $\alpha$ -synuclein fibril formation, *J. Biol. Chem.* 276 (2001) 10737–10744.
- [6] K.A. Conway, J.D. Harper, P.T. Lansbury, Accelerated in vitro fibril formation by a mutant  $\alpha$ -synuclein linked to early-onset Parkinson disease, *Nat. Med.* 4 (1998) 1318–1320.
- [7] V.H. FINDER, R. Glockshuber, Amyloid- $\beta$  aggregation, *Neurodegener. Dis.* 4 (2007) 13–27.
- [8] N.K. Holm, S.K. Jespersen, L.V. Thomassen, T.Y. Wolff, P. Sehgal, L.A. Thomsen, G. Christiansen, C.B. Andersen, A.D. Knudsen, D.E. Otzen, Aggregation and fibrillation of bovine serum albumin, *Biochim. Biophys. Acta* 1774 (2007) 1128–1138.
- [9] D.F. Waugh, Reactions involved in insulin fibril formation, *Fed. Proc.* 5 (1946) 111.
- [10] F. Gejyo, T. Yamada, S. Odani, Y. Nakagawa, M. Arakawa, T. Kunitomo, H. Kataoka, M. Suzuki, Y. Hirasawa, T. Shirahama, et al., A new form of amyloid protein associated with chronic hemodialysis was identified as  $\beta$ 2-microglobulin, *Biochem. Biophys. Res. Commun.* 129 (1985) 701–706.
- [11] P.B. Stathopoulos, J.A. Rummelt, G.A. Scholz, R.A. Irani, H.E. Frey, R.A. Hallowell, J.R. Lepock, E.M. Meiering, Cu/Zn superoxide dismutase mutants associated with amyotrophic lateral sclerosis show enhanced formation of aggregates in vitro, *Proc. Natl. Acad. Sci. USA* 100 (2003) 7021–7026.
- [12] P. Westermark, C. Wernstedt, E. Wilander, D.W. Hayden, T.D. O'Brien, K.H. Johnson, Amyloid fibrils in human insulinoma and islets of Langerhans of the diabetic cat are derived from a neuro-peptide-like protein also present in normal islet cells, *Proc. Natl. Acad. Sci. USA* 84 (1987) 3881–3885.
- [13] F. Ding, J.M. Borreguero, S.V. Buldyreva, H.E. Stanley, N.V. Dokholyan, Mechanism for the  $\alpha$ -helix to  $\beta$ -hairpin transition, *Proteins* 53 (2003) 220–228.
- [14] S. Singh, C.C. Chiu, A.S. Reddy, J.J. de Pablo,  $\alpha$ -helix to  $\beta$ -hairpin transition of human amylin monomer, *J. Chem. Phys.* 138 (2013) 155101.
- [15] A. Abedini, D.P. Raleigh, A critical assessment of the role of helical intermediates in amyloid formation by natively unfolded proteins and polypeptides, *Protein Eng. Des. Sel.* 22 (2009) 453–459.
- [16] V.L. Anderson, T.F. Ramlall, C.C. Rospigliosi, W.W. Webb, D. Eliezer, Identification of a helical intermediate in trifluoroethanol-induced  $\alpha$ -synuclein aggregation, *Proc. Natl. Acad. Sci. USA* 107 (2010) 18850–18855.
- [17] V.L. Anderson, W.W. Webb, A desolvation model for trifluoroethanol-induced aggregation of enhanced green fluorescent protein, *Biophys. J.* 102 (2012) 897–906.
- [18] I. Pallares, J. Vendrell, F.X. Aviles, S. Ventura, Amyloid fibril formation by a partially structured intermediate state of  $\alpha$ -chymotrypsin, *J. Mol. Biol.* 342 (2004) 321–331.
- [19] S. Srisailem, H.M. Wang, T.K.S. Kumar, D. Rajalingam, V. Sivaraja, H.S. Sheu, Y.C. Chang, C. Yu, Amyloid-like fibril formation in an all  $\beta$ -barrel protein involves the formation of partially structured intermediate(s), *J. Biol. Chem.* 277 (2002) 19027–19036.
- [20] F. Casallanovo, F.J. de Oliveira, F.C. de Souza, U. Ros, Y. Martinez, D. Penton, M. Tejuca, D. Martinez, F. Pazos, T.A. Pertinhez, A. Spisni, E.M. Cilli, M.E. Lania, C. Alvarez, S. Schreier, Model peptides mimic the structure and function of the N-terminus of the pore-forming toxin sticholysin II, *Biopolymers* 84 (2006) 169–180.

- [21] D.V. Waterhous, W.C. Johnson Jr., Importance of environment in determining secondary structure in proteins, *Biochemistry* 33 (1994) 2121–2128.
- [22] N.K. Bhatia, S. Deep, Diagnostic tools for structural characterization and elucidation of fibrils and their precursors in amyloid fibril formation pathway, *J. Protein Proteom.* 4 (2013) 149–164.
- [23] H. LeVine 3rd, Thioflavine T interaction with synthetic Alzheimer's disease beta-amyloid peptides: detection of amyloid aggregation in solution, *Protein Sci.* 2 (1993) 404–410.
- [24] J.S. Richardson, D.C. Richardson, Natural beta-sheet proteins use negative design to avoid edge-to-edge aggregation, *Proc. Natl. Acad. Sci. USA* 99 (2002) 2754–2759.
- [25] C.H. Trinh, D.P. Smith, A.P. Kalverda, S.E. Phillips, S.E. Radford, Crystal structure of monomeric human beta-2-microglobulin reveals clues to its amyloidogenic properties, *Proc. Natl. Acad. Sci. USA* 99 (2002) 9771–9776.
- [26] D. Roccatano, G. Colombo, M. Fioroni, A.E. Mark, Mechanism by which 2,2,2-trifluoroethanol/water mixtures stabilize secondary-structure formation in peptides: a molecular dynamics study, *Proc. Natl. Acad. Sci. USA* 99 (2002) 12179–12184.